

Calculation of the Antiferromagnetic Coupling and the Absorption Spectra of the Cation μ -Oxobis {pentammine-chromium(III)} by Means of Symmetry Parameters

JØRGEN GLERUP

Chemistry Department I (Inorganic Chemistry), University of Copenhagen, H. C. Ørsted Institute, Universitetsparken 5, DK-2100 Copenhagen Ø, Denmark

A model for calculation of the antiferromagnetic coupling and the absorption spectra (double excitation) has been developed. It is proved that there exists a one-electron matrix element between atomic orbitals situated at each of the chromium atoms. Through configuration interaction between the lowest levels and charge-transfer levels this matrix element gives the Landé interval rule for an antiferromagnetic coupling with the singlet as ground state. Furthermore it mixes doubly excited levels with allowed one-electron charge-transfer levels, whereby transitions to doubly excited levels become allowed.

Low temperature glass spectra of the basic rhodo ion have been measured. The observed absorption bands and the antiferromagnetic coupling in the ground state are compared with the calculated results of a three parameter model.

Several papers¹⁻⁶ are dealing with pair bands in antiferromagnetically coupled dinuclear complexes, but the origin of the antiferromagnetic coupling and the intensity of the pair bands are not understood. We will here discuss the cation μ -oxobis{pentamminechromium(III)} (called basic rhodo⁷) particularly because of its unusual absorption spectrum.

There have been conflicting reports^{8,9} of the magnetic susceptibility of $[(\text{NH}_3)_5\text{CrO}(\text{Cr}(\text{NH}_3)_5)\text{Cl}_4 \cdot \text{H}_2\text{O}]$ in the literature. This has now been elucidated by Pedersen¹⁰ who has shown that the magnetic susceptibility measurements are in accordance with an intramolecular spin-spin coupling between two entities with $S = \frac{3}{2}$ and with a triplet-singlet separation of $450 \pm 2 \text{ cm}^{-1}$ with the singlet as ground state. The energies of the lowest levels are shown in Fig. 1, where J is the constant in the Heisenberg-Dirac-Van Vleck operator $J\mathcal{S}_a \cdot \mathcal{S}_b$.

If J were to be interpreted as a sum of two-centered exchange integrals the order of the levels would be opposed, because exchange integrals are positive. Furthermore two-centered exchange integrals in the dinuclear

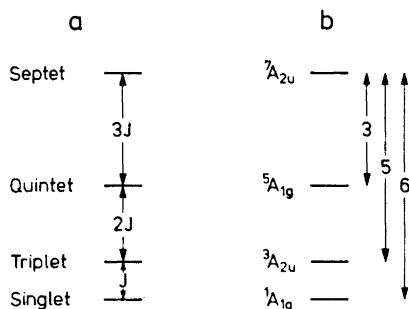


Fig. 1. a. Relative energies of lowest levels from the interpretation of magnetic susceptibility measurements by means of the operator $JS_a \cdot S_b$ where $J = 450 \text{ cm}^{-1}$.¹⁰ b. Relative energies of lowest levels interpreted by the present model.

copper(II) acetate have been estimated by Hansen and Ballhausen³ to be of the order of magnitude of 1 cm^{-1} .

For the dinuclear copper(II) acetate Jørgensen,¹¹ in order to explain the fact that the singlet in the antiferromagnetically coupled complex has a lower energy than the triplet, has proposed a one-electron interaction which mixes the singlet ground state with a charge-transfer state.

In the following we will discuss the more complicated case of basic rhodo where a similar model gives the non-trivial result that the Landé interval rule is obeyed.

EXPERIMENTAL

Preparation. 20 g $[(\text{NH}_3)_5\text{CrOHCr}(\text{NH}_3)_5](\text{ClO}_4)_6 \cdot 3\text{H}_2\text{O}$ ¹² and 20 g potassium trifluoroacetate were suspended in 10 ml water acidified with a drop of trifluoroacetic acid. Under stirring 50 ml ethanol was added and after 30 min the potassium perchlorate was filtered off. The complex was precipitated by slow addition of 200 ml ether. It was recrystallized twice by dissolving in 95 % ethanol and precipitating with ether. Yield 11 g needle shaped orange crystals. (Found: Cr 11.44; C 13.28; NH_3 18.80. Calc. for $[(\text{NH}_3)_5\text{CrOHCr}(\text{NH}_3)_5](\text{CF}_3\text{COO})_6 \cdot 3\text{H}_2\text{O}$: Cr 11.42; C 13.19; NH_3 18.71.)

The half life of basic rhodo at room temperature is 44 sec.¹³ Therefore the complex was not isolated but prepared in the cold just before the measurement.

Low temperature absorption spectra in the 210–1800 nm region were recorded on a Cary Model 14 spectrophotometer using a low temperature cuvette constructed in this laboratory by S. E. Harnung. The temperature was measured with a nickel-chromium/nickel thermocouple relative to liquid nitrogen boiling at 760 torr.

The solution was made as follows: A suspension (or solution depending on the concentration) of $[(\text{NH}_3)_5\text{CrOHCr}(\text{NH}_3)_5](\text{CF}_3\text{COO})_6 \cdot 3\text{H}_2\text{O}$ in 4:1 absolute ethanol-methanol mixture was cooled to -60°C , and 1/20 volume of the 4:1 ethanol-methanol mixture saturated with sodium hydroxide was added to the solution.

The concentration was estimated at different temperatures with the formula found by Passerini¹⁴ $V_{20}^t = 1 + 1.125 \times 10^{-3} (t - 20) + 1.11 \times 10^{-6} (t - 20)^2$.

ABSORPTION SPECTRA

The absorption spectrum of basic rhodo was measured some ten years ago by Schäffer¹⁵ and has later been measured by several other authors.^{10,13,16,17} The low temperature glass spectra shown in Fig. 2 have been measured in an ethanol–methanol mixture at temperatures of 230 K and 121 K. The two broad

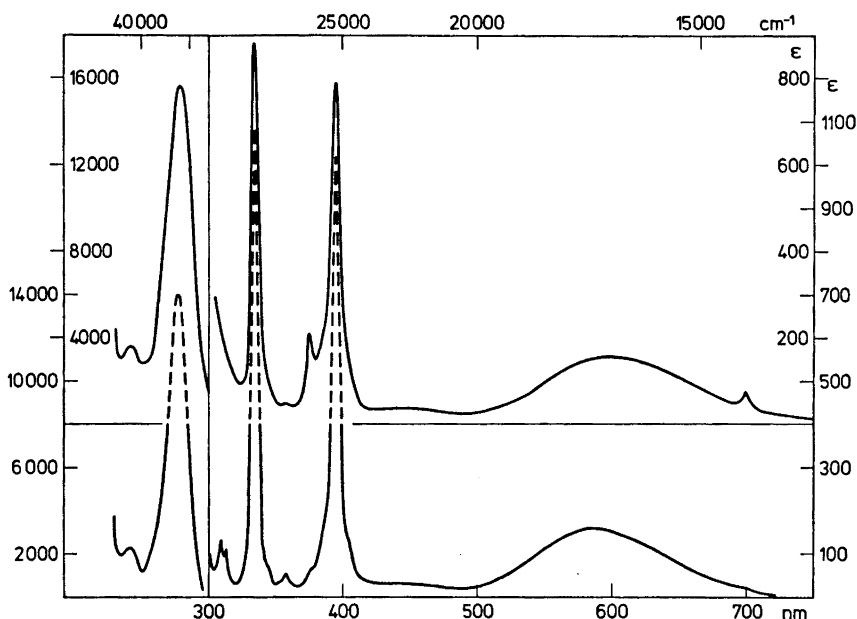


Fig. 2. Absorption spectra of $[(\text{NH}_3)_5\text{CrOCr}(\text{NH}_3)_5]^{4+}$ in 4:1 ethanol-methanol mixture. The upper curve is measured at 230 K and the lower curve at 121 K.

bands at $22\,500\text{ cm}^{-1}$ and $16\,800\text{ cm}^{-1}$ resemble the spin-allowed bands observed in mononuclear chromium(III) complexes. The two weak bands at $14\,290\text{ cm}^{-1}$ and $26\,660\text{ cm}^{-1}$ are hot bands as found by Dubicki and Martin.¹⁶ Their intensities vary in accordance with a Boltzmann factor $e^{-E/kT}$ with $E = 450\text{ cm}^{-1}$ where E is the triplet-singlet separation. This means that the hot bands are transitions from the lowest populated triplet to some excited triplet.

The temperature dependence of the intensities of the other sharp bands shows that they are allowed transitions because they become sharper and slightly more intense on cooling. These bands are transitions from the singlet ground state to some excited singlet states.

We first considered the sharp bands as double excitation of doublets which were coupled by $JS_a \cdot S_b$. We chose this mechanism because it is well known¹⁸ that the only sharp bands in mononuclear chromium(III) complexes are due to spin-forbidden transitions to excited states with the same cubic parentage subconfiguration as the ground state.

Since the coupling of two doublets gives rise to singlets and triplets, transitions to these levels from the singlet ground state become spin-allowed. The reason for the allowedness of transitions to such doubly excited levels will be discussed later. Coupling of doublets with quartets gives triplets and quintets which means that spin-allowed transitions to these levels will be hot bands.

THEORETICAL PART

The basic rhodo ion has D_{4h} symmetry.^{10,19-20} For a tetragonal chromophore we define the one-electron parameters²¹ as

$$\Delta = \frac{1}{2}[\hbar(\theta) + \hbar(\varepsilon)] - \frac{1}{3}[\hbar(\xi) + \hbar(\eta) + \hbar(\zeta)]$$

$$\Delta(e) = \hbar(\varepsilon) - \hbar(\theta); \Delta(t_2) = \hbar(\zeta) - \hbar(\xi) = \hbar(\zeta) - \hbar(\eta)$$

where

$$\theta = z^2 - \frac{1}{2}x^2 - \frac{1}{2}y^2, \varepsilon = \frac{\sqrt{3}}{2}(x^2 - y^2), \zeta = \sqrt{3}xy, \xi = \sqrt{3}yz$$

and

$$\eta = \sqrt{3}zx$$

Following the angular overlap model²² it is assumed that the splitting $\Delta(t_2)$ is due to differences in the ability of NH_3 and O to form π -bonding to the chromium

$$\Delta(t_2) = \frac{1}{4}(\Delta_{\pi\text{NH}_3} - \Delta_{\pi\text{O}})$$

Because the perturbation from the oxygen atom is distributed on the two chromium atoms, the perturbation on a single chromium atom is called $\Delta_{\pi\text{O}}$.

In the model δ -bonds are neglected and it is assumed that NH_3 is unable to form π -bonds with the metal.

In Fig. 3 the p_y orbital on the oxygen atom and the ξ orbital on each of the chromium atoms have been drawn. It is seen that the negative linear combination $\xi_b - \xi_a$ of the atomic orbitals interacts with the p_y orbital on oxygen while the positive linear combination cannot interact, the same is true for the linear combinations of the η orbitals. Neither the positive nor the negative linear combination of ζ orbitals is able to interact with any of the

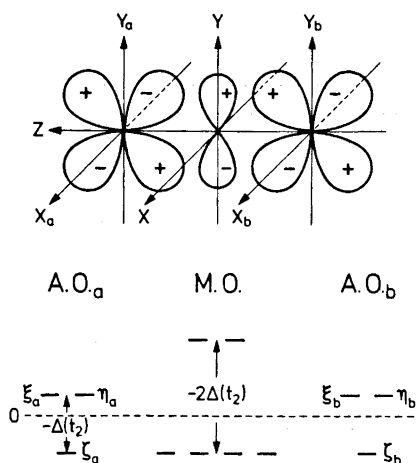


Fig. 3. The figure shows the ξ_a orbital on metal a, the ξ_b orbital on metal b and the p_y orbital on the oxygen.

Below the drawing the relative energies of the t_2 orbitals are shown on each side of the molecular orbitals.

oxygen orbitals. In the angular overlap model all the noninteracting orbitals must have the same energy

$$\hbar\left(\frac{1}{\sqrt{2}}(\xi_b + \xi_a)\right) = \hbar\left(\frac{1}{\sqrt{2}}(\eta_b + \eta_a)\right) = \hbar\left(\frac{1}{\sqrt{2}}(\zeta_b + \zeta_a)\right) = \hbar\left(\frac{1}{\sqrt{2}}(\zeta_b - \zeta_a)\right) = \frac{2}{3}\Delta(t_2)$$

where the zero point has been chosen so that the one-electron energy for the t_2^3 configuration is zero.

The baricenter rule gives the energy of the negative linear combination of the atomic orbitals (see Fig. 3)

$$\hbar\left(\frac{1}{\sqrt{2}}(\xi_b - \xi_a)\right) = \hbar\left(\frac{1}{\sqrt{2}}(\eta_b - \eta_a)\right) = -\frac{1}{3}\Delta(t_2) - \Delta(t_2) = -\frac{4}{3}\Delta(t_2)$$

Then we have the following matrix equation which can be rediagonalized to a matrix equation with atomic orbitals.

$$\begin{array}{cc|cc} \frac{1}{\sqrt{2}}(\xi_b - \xi_a) & -\frac{4}{3}\Delta(t_2) & 0 & \\ \frac{1}{\sqrt{2}}(\xi_b + \xi_a) & 0 & \frac{2}{3}\Delta(t_2) & \end{array} \longrightarrow \begin{array}{cc|cc} \xi_a & -\frac{1}{3}\Delta(t_2) & \Delta(t_2) & \\ \xi_b & \Delta(t_2) & -\frac{1}{3}\Delta(t_2) & \end{array}$$

The last equation shows that there exists a one-electron matrix element between atomic orbitals centered on each of the chromium atoms with the size $\langle \xi_a | V | \xi_b \rangle = \langle \eta_a | V | \eta_b \rangle = \Delta(t_2)$ where V is the ligand field operator. In deriving this the overlap integral $\langle \xi_a | \xi_b \rangle$ is considered to be small, but of course the overlap integral $\langle (1/\sqrt{2})(\xi_b - \xi_a) | p_y \rangle$ is not small.

Fig. 3 also shows the molecular orbitals. These are filled with the six electrons in such a way that there is only one electron in each orbital and for the septet the spins are aligned. This is not in accordance with the original proposal of Dunitz and Orgel²³ who neglected the electron repulsion within each of the chromium atoms.

With the matrix element $\langle \xi_a | V | \xi_b \rangle = \Delta(t_2)$ we are now able to calculate the absorption spectra and the antiferromagnetic coupling.

In the model the following Hamilton operator has been used.

$$H = V_a + \sum_{i < j}^a \frac{e^2}{r_{ij}} + V_b + \sum_{i < j}^b \frac{e^2}{r_{ij}} + V_{ab}$$

where V_a is the ligand field operator of atom a and where V_{ab} is the one electron interaction operator whose consequences we have just derived.* In the operator a two-centered repulsion term is omitted because two-centered repulsion integrals are considered to be small.

As starting functions we have used linear combinations of Slater determinants of the t_2^3 sub-configuration in C_{4v} symmetry from Griffith's book²⁴ which are solutions to the first part of the Hamilton operator $V + \sum_{i < j}^e \frac{e^2}{r_{ij}}$. The functions for each of the chromium atoms have been coupled together

* The perturbation from the oxygen atom gives rise to the three terms $V_a + V_b + V_{ab}$.

simply by coupling the spins (tables of vector coupling coefficients were taken from Heine ²⁵) and taking the products of the orbital parts. For the lowest levels we obtain ${}^4B_1({}^4A_2) \times {}^4B_1({}^4A_2) = {}^1A_{1g}(D_{4h}) + {}^3A_{2u}(D_{4h}) + {}^5A_{1g}(D_{4h}) + {}^7A_{2u}(D_{4h})$, where ${}^4B_1({}^4A_2)$ is the ground state of t_2^3 in C_{4v} symmetry and the symbol in parenthesis is the ground state in octahedral symmetry. The energy separation between the obtained levels caused by the two-centered exchange integrals are small.³

The antiferromagnetic coupling. Under the one-electron operator, configuration interaction between the lowest levels and charge-transfer levels gives the Landé interval rule for the lowest levels.

Lowest levels

$$[t_2^3 {}^4B_1({}^4A_2)] \times [t_2^3 {}^4B_1({}^4A_2)] = {}^1A_{1g} + {}^3A_{2u} + {}^5A_{1g} + {}^7A_{2u}(D_{4h})$$

Charge-transfer levels

$$[t_2^2 {}^3E({}^3T_1)] \times [t_2^4 {}^3E({}^3T_1)] = {}^1A_{1g} + {}^3A_{2u} + {}^5A_{1g}(D_{4h}) \text{ and others.}$$

The complete functions written as linear combination of Slater determinants are listed in Table 1.

These charge transfer levels are the only ones which have non-diagonal elements with the lowest levels and as long as two-centered exchange integrals are neglected the three levels have the same energy.

Table 1. The functions for the lowest levels and the charge-transfer levels written as linear combination of Slater determinants. A bar indicates an orbital with β spin.

Lowest levels

$${}^7A_{2u} \quad |\xi_a \eta_a \zeta_a \bar{\xi}_b \eta_b \bar{\zeta}_b|$$

$${}^5A_{1g} \quad \frac{1}{\sqrt{6}} |\xi_a \eta_a \zeta_a (\bar{\xi}_b \eta_b \bar{\zeta}_b + \bar{\xi}_b \eta_b \bar{\zeta}_b + \bar{\xi}_b \eta_b \bar{\zeta}_b) - (\bar{\xi}_a \eta_a \zeta_a + \xi_a \bar{\eta}_a \bar{\zeta}_a + \xi_a \eta_a \bar{\zeta}_a) \bar{\xi}_b \eta_b \bar{\zeta}_b|$$

$${}^3A_{2u} \quad \frac{1}{\sqrt{10}} |\xi_a \eta_a \zeta_a (\bar{\xi}_b \eta_b \bar{\zeta}_b + \bar{\xi}_b \eta_b \bar{\zeta}_b + \bar{\xi}_b \eta_b \bar{\zeta}_b) - \frac{2}{3} (\bar{\xi}_a \eta_a \zeta_a + \xi_a \eta_a \bar{\zeta}_a + \xi_a \eta_a \bar{\zeta}_a) (\bar{\xi}_b \eta_b \bar{\zeta}_b + \bar{\xi}_b \eta_b \bar{\zeta}_b + \bar{\xi}_b \eta_b \bar{\zeta}_b) + (\bar{\xi}_a \eta_a \zeta_a + \bar{\xi}_a \eta_a \bar{\zeta}_a + \xi_a \eta_a \bar{\zeta}_a) \bar{\xi}_b \eta_b \bar{\zeta}_b|$$

$${}^1A_{1g} \quad \frac{1}{2} |\xi_a \eta_a \zeta_a \bar{\xi}_b \eta_b \bar{\zeta}_b - \frac{1}{3} (\bar{\xi}_a \eta_a \zeta_a + \xi_a \bar{\eta}_a \bar{\zeta}_a + \xi_a \eta_a \bar{\zeta}_a) (\bar{\xi}_b \eta_b \bar{\zeta}_b + \bar{\xi}_b \eta_b \bar{\zeta}_b + \bar{\xi}_b \eta_b \bar{\zeta}_b) + \frac{1}{3} (\bar{\xi}_a \eta_a \zeta_a + \bar{\xi}_a \eta_a \bar{\zeta}_a + \xi_a \eta_a \bar{\zeta}_a) (\bar{\xi}_b \eta_b \bar{\zeta}_b + \bar{\xi}_b \eta_b \bar{\zeta}_b + \bar{\xi}_b \eta_b \bar{\zeta}_b) - \xi_a \bar{\eta}_a \bar{\zeta}_a \bar{\xi}_b \eta_b \bar{\zeta}_b|$$

Charge-transfer levels

$${}^5A_{1g} \quad \frac{1}{2} |\zeta_a \eta_a \bar{\xi}_b \bar{\xi}_b \eta_b \bar{\zeta}_b - \xi_a \bar{\zeta}_a \bar{\xi}_b \eta_b \bar{\zeta}_b + \xi_a \bar{\xi}_a \eta_a \bar{\zeta}_a \bar{\xi}_b \eta_b - \xi_a \eta_a \bar{\xi}_a \bar{\xi}_b \bar{\zeta}_b|$$

$${}^3A_{2u} \quad \frac{1}{2} |\zeta_a \eta_a (\bar{\xi}_b \bar{\xi}_b \eta_b \bar{\zeta}_b + \bar{\xi}_b \bar{\xi}_b \eta_b \bar{\zeta}_b) - (\bar{\zeta}_a \eta_a + \zeta_a \bar{\eta}_a) \bar{\xi}_b \bar{\xi}_b \eta_b \bar{\zeta}_b - \xi_a \bar{\zeta}_a (\bar{\xi}_b \eta_b \bar{\zeta}_b + \bar{\xi}_b \eta_b \bar{\zeta}_b) + (\bar{\xi}_a \bar{\zeta}_a + \xi_a \bar{\zeta}_a) \bar{\xi}_b \eta_b \bar{\zeta}_b + \xi_a \bar{\xi}_a \eta_a \bar{\zeta}_a (\bar{\xi}_b \eta_b + \bar{\zeta}_b \eta_b) - (\xi_a \bar{\xi}_a \eta_a \bar{\zeta}_a + \xi_a \bar{\xi}_a \eta_a \bar{\zeta}_a) \bar{\zeta}_b \eta_b - \xi_a \eta_a \bar{\xi}_a \bar{\zeta}_a (\bar{\xi}_b \bar{\zeta}_b + \bar{\xi}_b \bar{\zeta}_b) + (\bar{\xi}_a \eta_a \bar{\xi}_a \bar{\zeta}_a + \xi_a \eta_a \bar{\xi}_a \bar{\zeta}_a) \bar{\xi}_b \bar{\zeta}_b|$$

$${}^1A_{1g} \quad \frac{1}{2\sqrt{3}} |\zeta_a \eta_a \bar{\xi}_b \bar{\xi}_b \eta_b \bar{\zeta}_b - \frac{1}{2} (\bar{\zeta}_a \eta_a + \zeta_a \bar{\eta}_a) (\bar{\xi}_b \bar{\xi}_b \eta_b \bar{\zeta}_b + \bar{\xi}_b \bar{\xi}_b \eta_b \bar{\zeta}_b) + \bar{\zeta}_a \bar{\xi}_a \bar{\xi}_b \bar{\xi}_b \eta_b \bar{\zeta}_b - \xi_a \bar{\zeta}_a \bar{\xi}_b \eta_b \bar{\zeta}_b + \frac{1}{2} (\bar{\xi}_a \bar{\zeta}_a + \xi_a \bar{\zeta}_a) (\bar{\xi}_b \eta_b \bar{\zeta}_b + \bar{\xi}_b \eta_b \bar{\zeta}_b) - \bar{\xi}_a \bar{\zeta}_a \bar{\xi}_b \eta_b \bar{\zeta}_b + \xi_a \bar{\xi}_a \eta_a \bar{\zeta}_a \bar{\xi}_b \eta_b - \frac{1}{2} (\bar{\xi}_a \bar{\xi}_a \eta_a \bar{\zeta}_a + \xi_a \bar{\xi}_a \eta_a \bar{\zeta}_a) (\bar{\xi}_b \eta_b + \bar{\zeta}_b \eta_b) + \xi_a \bar{\xi}_a \eta_a \bar{\zeta}_a \bar{\xi}_b \eta_b - \xi_a \eta_a \bar{\xi}_a \bar{\zeta}_a \bar{\xi}_b \bar{\zeta}_b + \frac{1}{2} (\bar{\xi}_a \eta_a \bar{\xi}_a \bar{\zeta}_a + \xi_a \eta_a \bar{\xi}_a \bar{\zeta}_a) (\bar{\xi}_b \bar{\zeta}_b + \bar{\xi}_b \bar{\zeta}_b) - \bar{\xi}_a \eta_a \bar{\xi}_a \bar{\zeta}_a \bar{\xi}_b \bar{\zeta}_b|$$

Table 2. The ${}^1E_u(D_{4h})$ matrix. The functions are labelled 1 to 18. Most of the non-diagonal elements are given in the scheme, where all the numbers are coefficients to the factor $\frac{1}{2\sqrt{6}}\Delta(t_2)$. $f_0 = A + B + 2C$ and $f_4 = 3B + C$.

${}^1E_u(D_{4h})$ matrix	Function Diagonal number elements	Non-diagonal elements							
$[t_2^3 A_1 ({}^2E)] \times [t_2^3 E ({}^2T_1)]$	1 $6f_2$	3	$-\sqrt{3}$	3	$-\sqrt{3}$	3	$-\sqrt{3}$	3	$-\sqrt{3}$
$[t_2^3 B_1 ({}^2E)] \times [t_2^3 E ({}^2T_1)]$	2 $6f_4$								
$[t_2^3 A_1 ({}^3E)] \times [t_2^3 E ({}^3T_2)]$	3 $8f_4$	(1,3) = (2,4) = (5,7) = (6,8) = $-\Delta(t_2)$							
$[t_2^3 B_1 ({}^3E)] \times [t_2^3 E ({}^3T_2)]$	4 $8f_2$	(11,12) = $\frac{2\sqrt{2}}{3}\Delta(t_2)$							
$[t_2^3 A_2 ({}^2T_1)] \times [t_2^3 E ({}^2T_1)]$	5 $6f_2$	(15,16) = $-\frac{2\sqrt{2}}{3}\Delta(t_2)$							
$[t_2^3 B_2 ({}^2T_2)] \times [t_2^3 E ({}^2T_1)]$	6 $8f_2$								
$[t_2^3 A_1 ({}^2T_1)] \times [t_2^3 E ({}^2T_2)]$	7 $8f_2$								
$[t_2^3 B_2 ({}^2T_2)] \times [t_2^3 E ({}^2T_2)]$	8 $10f_2$								
$[t_2^3 A_2 ({}^3T_1)] \times [t_2^3 E ({}^3T_1)]$	9 $f_0 + 3f_2 - \Delta(t_2)$								
$[t_2^3 E ({}^3T_1)] \times [t_2^3 A_2 ({}^3T_1)]$	10 $f_0 + 3f_2 + \Delta(t_2)$								
$[t_2^3 E ({}^1T_1)] \times [t_2^4 A_1 ({}^1A_1)]$	11 $f_0 + 10f_2 + \frac{1}{3}\Delta(t_2)$								
$[t_2^3 E ({}^1T_1)] \times [t_2^4 A_1 ({}^1E)]$	12 $f_0 + 7f_2 + \Delta(t_2)$								
$[t_2^3 E ({}^1T_1)] \times [t_2^4 B_1 ({}^1E)]$	13 $f_0 + 7f_2 + \Delta(t_2)$								
$[t_2^3 E ({}^1T_1)] \times [t_2^4 B_2 ({}^1T_2)]$	14 $f_0 + 7f_2 + \Delta(t_2)$								
$[t_2^3 A_1 ({}^1A_1)] \times [t_2^4 E ({}^1T_1)]$	15 $f_0 + 10f_2 - \frac{1}{3}\Delta(t_2)$								
$[t_2^3 A_1 ({}^1E)] \times [t_2^4 E ({}^1T_1)]$	16 $f_0 + 7f_2 + \frac{1}{3}\Delta(t_2)$								
$[t_2^3 B_1 ({}^1E)] \times [t_2^4 E ({}^1T_1)]$	17 $f_0 + 7f_2 - \Delta(t_2)$								
$[t_2^3 B_2 ({}^1E)] \times [t_2^4 E ({}^1T_1)]$	18 $f_0 + 7f_2 - \Delta(t_2)$								

The non-diagonal matrix elements for levels with the same symmetry are

$$\begin{aligned}\langle {}^1A_{1g} | V_{ab} | {}^1A_{1g} \text{ c.t.} \rangle &= -\frac{4}{\sqrt{3}} \Delta(t_2) \\ \langle {}^3A_{2u} | V_{ab} | {}^3A_{2u} \text{ c.t.} \rangle &= -\frac{2\sqrt{10}}{3} \Delta(t_2) \\ \langle {}^5A_{1g} | V_{ab} | {}^5A_{1g} \text{ c.t.} \rangle &= -\frac{4}{\sqrt{6}} \Delta(t_2)\end{aligned}$$

The lowest levels have the same energy but after the configuration interaction with the charge transfer levels, the energy of the septet is unaltered, the energy of the quintet is lowered by

$$\frac{[-(4/\sqrt{6})\Delta(t_2)]^2}{E_{\text{c.t.}}} = \frac{8}{3} \frac{[\Delta(t_2)]^2}{E_{\text{c.t.}}}, \text{ the energy of the triplet by } \frac{4}{9} \frac{[\Delta(t_2)]^2}{E_{\text{c.t.}}}$$

and the energy of the singlet is lowered by $\frac{1}{3} \frac{[\Delta(t_2)]^2}{E_{\text{c.t.}}}$.

The ratios between the changes in energy are $\frac{8}{3} : \frac{4}{9} : \frac{1}{3} = 3:5:6$, which is just the Landé interval rule for an antiferromagnetic coupling (Fig. 1).

With $\Delta(t_2) \cong -4000 \text{ cm}^{-1}$ and a septet singlet separation of 2700 cm^{-1} from experiments $E_{\text{c.t.}}$ becomes $E_{\text{c.t.}} = \frac{16(-4000)^2}{3 \cdot 2700} \cong 32000 \text{ cm}^{-1}$. This is a very low energy for a charge-transfer state where an electron is moved from one chromium atom to the other. But it is in accordance with the observed absorption band at 35940 cm^{-1} with an absorbancy of $16000 \text{ cm}^2/\text{mol}$. In mononuclear complexes no similar absorption band is observed and because of the high absorbancy it is interpreted as a charge-transfer band.

From the above discussion we conclude that antiferromagnetic couplings in dimeric systems are caused by a one-electron interaction between atomic orbitals situated at each metal atom which mix the lowest levels with charge-transfer levels.

Calculation of spectra. In the calculations of the absorption spectra all the functions of the t_2^3 configuration in C_{4v} symmetry have been coupled $\{ {}^4B_1({}^4A_2), {}^2A_1({}^2E), {}^2B_1({}^2E), {}^2E({}^2T_1), {}^2A_2({}^2T_1), {}^2E({}^2T_2) \text{ and } {}^2B_2({}^2T_2) \} \times \{ \text{the same functions} \}$. For the charge-transfer levels all the states of the t_2^2 configuration have been coupled with all the states of the t_2^4 configuration.

$$\begin{aligned}\{ & {}^3E({}^3T_1 t_2^2), {}^3A_2({}^3T_1 t_2^2), {}^1E({}^1T_2 t_2^2), {}^1B_2({}^1T_2 t_2^2), {}^1A_1({}^1A_1 t_2^2), \\ & {}^1A_1({}^1E t_2^2) \text{ and } {}^1B_1({}^1E t_2^2) \} \times \{ {}^3E({}^3T_1 t_2^4), {}^3A_2({}^3T_1 t_2^4), {}^1E({}^1T_2 t_2^4), \\ & {}^1B_2({}^1T_2 t_2^4), {}^1A_1({}^1A_1 t_2^4), {}^1A_1({}^1E t_2^4) \text{ and } {}^1B_1({}^1E t_2^4) \}\end{aligned}$$

The matrices which contain the four lowest levels were calculated: ${}^7A_{2u}(1)$, ${}^5A_{1g}(3)$, ${}^3A_{2u}(9)$ and ${}^1A_{1g}(7)$, where the numbers in parenthesis are the orders of the matrices. Furthermore the matrices to which electrical dipole transitions from the lowest levels ${}^1A_{1g}$ and ${}^3A_{2u}$ are allowed were calculated: ${}^1E_u(18)$, ${}^1A_{2u}(10)$, ${}^3E_g(22)$ and ${}^3A_{1g}(6)$. The matrix 1E_u is given in Table 2. In the matrices $\Delta(t_2)$ is the only non-diagonal parameter. The diagonal energies for

double excitation is simply the sum of the single excitation energies. The energies were expressed in Racah parameters and the ligand field parameter $\Delta(t_2)$. The energies of charge-transfer levels were also expressed in Racah parameters, *i.e.* the diagonal energy for the charge-transfer levels $[t_2^2 {}^3E({}^3T_1)] \times [t_2^4 {}^3E({}^3T_1)]$ which interacts with the lowest levels is

$$(A - 5B + \frac{1}{3}\Delta(t_2)) + (6A - 15B + 5C - \frac{1}{3}\Delta(t_2)) - 2(3A - 15B) = A + 10B + 5C = f_0 + 3f_2$$

where $-2(3A - 15B)$ arises because the energy of ${}^7A_{2u}$ from $[t_2^3 {}^4B_1({}^4A_2)] \times [t_2^3 {}^4B_1({}^4A_2)]$ has been chosen as zero point. This makes it possible to determine the Racah parameter A . Configuration interaction with the e -orbitals has been neglected (otherwise the size of the matrices would have been enormous). Therefore the three parameters become linearly dependent, and they have been replaced by two new parameters $f_0 = A + B + 2C$ and $f_2 = 3B + C$.

Oscillator strengths. There are two charge-transfer levels of 1E_u symmetry to which transitions from the ground state ${}^1A_{1g}$ are allowed. The oscillator strength of the transitions is proportional to $|(-4/\sqrt{6})\langle \zeta_a | \vec{E} | \eta_b \rangle|^2$ and $|(-4/\sqrt{6})\langle \eta_a | \vec{E} | \zeta_b \rangle|^2$, where \vec{E} is the electrical dipole operator.

The oscillator strength for the allowed transitions from ${}^3A_{2u}$ to the two charge-transfer levels in the 3E_g matrix is proportional to $|(-2\sqrt{5}/3)\langle \zeta_a | \vec{E} | \eta_b \rangle|^2 3e^{-450 \text{ cm}^{-1}/kT}$ and $|(-2\sqrt{5}/3)\langle \eta_a | \vec{E} | \zeta_b \rangle|^2 3e^{-450 \text{ cm}^{-1}/kT}$. The ratio between the oscillator strengths of the triplet-triplet and the singlet-singlet transitions is therefore $\frac{5}{6} 3e^{-450 \text{ cm}^{-1}/kT}$.

The non-diagonal element $\Delta(t_2)$ mixes the charge-transfer levels with doubly excited levels, whereby transitions to the latter become allowed and the oscillator strength is proportional to $[\Delta(t_2)]^2/(E_{\text{c.t.}} - E_{\text{d.e.}})$ where $E_{\text{c.t.}} - E_{\text{d.e.}}$ is the difference in diagonal energies between the charge-transfer levels and the doubly excited levels.

In compounds where $E_{\text{c.t.}} \gg E_{\text{d.e.}}$ the oscillator strength for a transition to a doubly excited level will be proportional to J (the experimentally estimated constant in the operator $JS_a \cdot S_b$) because J is proportional to $[\Delta(t_2)]^2/E_{\text{c.t.}}$.

The charge-transfer band mentioned on p. 3782 is later assigned as a ${}^1A_{1g} \rightarrow {}^1A_{2u}$ transition, and the oscillator strength is proportional to $|(-4/\sqrt{3})\langle \eta_a | \vec{E} | \eta_b \rangle|^2$.

RESULTS

The three parameters have been varied in a weighted least squares model * to minimize the variance $\sum_{i=1}^N \frac{(E_{\text{obs } i} - E_{\text{calc } i})^2}{\sigma_{\text{obs } i}^2}$, where σ_{obs} is the standard deviation of the position of the absorption bands and N the number of observations. As standard deviation the halfwidth of the absorption bands was used,

* The program for handling the matrices and the statistical model has been written by cand. scient. Henrik Maegaard to whom we wish to express our gratitude. The program is written in Algol 6 for a RC 4000 computer but Henrik Maegaard has made a new edition for an IBM 360/75 computer.

Table 3. Observed and calculated absorption bands for the basic rhodo ion. The 450 cm⁻¹ in the first column is the ³A_{2u}-¹A_{1g} separation from the magnetic susceptibility measurements.¹⁰

Observed band positions cm ⁻¹	Half width σ _{obs} cm ⁻¹	Calculated cm ⁻¹	Assignment
14 290	500	13 680	³ A _{2u} → ³ E _g
26 660	500	26 826	³ A _{2u} → ³ E _g
25 340	500	25 042	¹ A _{1g} → ¹ E _u
29 890	400	30 501	¹ A _{1g} → ¹ E _u
31 930	500	31 169	¹ A _{1g} → ¹ E _u
32 340	500	32 797	¹ A _{1g} → ¹ E _u
35 940	2 800	35 726	¹ A _{1g} → ¹ A _{2u}
450	2	449.9	³ A _{2u} → ¹ A _{1g}
0		0	⁷ A _{2u}
- 1 350		- 1 443	⁵ A _{1g}
- 2 250		- 2 386	³ A _{2u}
- 2 700		- 2 836	¹ A _{1g}
Degrees of freedom: 8(obs.) - 3(param.) = 5			
Variance: 7.62			
χ ² test: 0.822			
Parameters: $f_0 = A + B + 2C = 17\,558\text{ cm}^{-1} \pm 620$			
$f_1 = 3B + C = 5\,111\text{ cm}^{-1} \pm 54$			
$\Delta(t_2) = -4\,221\text{ cm}^{-1} \pm 36$			

and as standard deviation for the ³A_{2u}-¹A_{1g} separation the value obtained from the magnetic measurements¹⁰ was used.

In Table 3 the observed and calculated band positions, the assignments, the variance, the degrees of freedom, and the χ² test are presented. Furthermore the standard deviations used for the band positions and the calculated parameters with standard deviations are given.

The agreement is rather satisfactory in spite of the fact that configuration interaction with *e*-orbitals has been neglected.

All the absorption bands are assigned as *A*→*E* transitions with the exception of the charge-transfer band at 35 940 cm⁻¹ which is assigned as a ¹A_{1g}-¹A_{2u} transition.

If this band is assigned as a ¹A_{1g}→¹E_u transition the χ² test gives 0.955 and we do not think this difference in the χ² test is conclusive, because the effect of the *e*-orbitals (which has not been incorporated) is not easy to predict. This ambiguity in the assignment could in principle be solved by measuring the polarized crystal spectra.

The assignment of the absorption bands as $A \rightarrow E$ transitions is confirmed by the polarized crystal spectra made by Akio Umshiyama,¹⁷ which show that all the sharp absorption bands in the visible and near ultraviolet region are forbidden in one direction of polarization. The $A \rightarrow E$ transitions are forbidden when the electric vector of the light waves is parallel to the molecular axis.

The calculated value for the parameter $f_2 = 3B + C = 5111 \text{ cm}^{-1}$ is very reasonable and the same is true of the parameter $\Delta(t_2) = \frac{1}{4}(\Delta_{\pi\text{NH}_3} - \Delta_{\pi_3\text{O}}) = -4221 \text{ cm}^{-1}$. For the ion $[\text{Cr}(\text{NH}_3)_6]^{3+}$ the parameter $3B + C$ is $3B + C \simeq 5100 \text{ cm}^{-1}$ (Ref. 24, Table 40). In *trans* $[(\text{Cr}(\text{NH}_3)_4(\text{OH})_2)]^+$ $\Delta(t_2)$ ²¹ is found to be $\Delta(t_2) = \frac{1}{2}(\Delta_{\pi\text{NH}_3} - \Delta_{\pi\text{OH}}) \simeq -4500 \text{ cm}^{-1}$, which means that the energy of the π -bonds formed by two hydroxo-groups are of the same order of magnitude as the π -bond formed by half an oxygen to one chromium(III) ion in basic rhodo.

The calculated value for the parameter $f_0 = A + B + 2C = 17558 \text{ cm}^{-1}$ is surprisingly low. Watson²⁶ has calculated the F^k integrals for the chromium(III) ion, and from these values the Racah parameter A should be $A \simeq 165 000 \text{ cm}^{-1}$. The inconsistency between these numbers is caused by the fact that the parameter A in the model is not really the Racah parameter A , mainly because the interaction between the d -electrons and the core electrons is not the same for a $d^3 - d^3$ as for a $d^2 - d^4$ system. Nevertheless it would appear that the parameter A gives a good description of the energy of the charge-transfer levels considered here.

In Table 4 are given all the observed band positions which were not incorporated in the calculations. Besides the two broad bands in the visible region a broad band at $41 460 \text{ cm}^{-1}$ is observed. These bands have not been incorporated in the calculations because we think they all involve the e -orbitals. Furthermore, several small absorption bands are observed especially at low temperatures. We believe that these bands are forbidden transitions and we have only concerned ourselves with the allowed transitions.

As a first approach, the sharp bands were characterized as transitions to doubly excited levels but because the value of the nondiagonal elements is rather big and the value of $f_0 = A + B + 2C$ is rather small, all the levels are highly mixed together so that the terminology doubly excited levels is not meaningful.

From the discussion on p. 3784 it should in principle be possible to calculate the ratios between the oscillator strengths of the absorption bands from the

Table 4. Observed absorption bands not incorporated in the calculations.

Broad bands, cm^{-1}	Sharp bands, cm^{-1}	
16 800	13 760	27 900
22 500	14 440	28 300
41 460	14 830	29 260
	24 730	29 540
	26 180	30 710

eigenvectors of the diagonalized matrices. For the absorption band 1E_u at 25 340 cm^{-1} the oscillator strength is proportional to:

$$0.0955^2 \left| -\frac{4}{\sqrt{6}} \langle \zeta_a | \vec{E} | \eta_b \rangle \right|^2 + 0.6476^2 \left| -\frac{4}{\sqrt{6}} \langle \eta_a | \vec{E} | \zeta_b \rangle \right|^2$$

and for the absorption band at 26 660 cm^{-1} assigned as a ${}^3A_{2u} \rightarrow {}^3E_g$ transition the oscillator strength is proportional to:

$$\left[0.1995^2 \left| -\frac{2\sqrt{5}}{3} \langle \zeta_a | \vec{E} | \eta_b \rangle \right|^2 + 0.3404^2 \left| -\frac{2\sqrt{5}}{3} \langle \eta_a | \vec{E} | \zeta_b \rangle \right|^2 \right] 3e^{-450 \text{ cm}^{-1}/kT}$$

Similar expressions can be constructed for the other absorption bands assigned as $A \rightarrow E$ transitions. The observed intensities do not fit the calculated oscillator strengths, *i.e.* the calculated intensities for the two ${}^3A_{2u} \rightarrow {}^3E_g$ transitions are too small and this is independent of the relative size of the two matrix elements $\langle \zeta_a | \vec{E} | \eta_b \rangle$ and $\langle \eta_a | \vec{E} | \zeta_b \rangle$. We attribute this lack of agreement to the fact that we have used a restricted set (only the t_2 -orbitals) in our calculations.

CONCLUSION

The present model explains the Landé interval rule in an antiferromagnetically coupled dinuclear complex as a one-electron interaction between atomic orbitals situated at each of the metal atoms which mixes the lowest levels with the charge-transfer levels. Furthermore, this matrix-element mixes doubly excited levels with allowed one-electron charge-transfer levels, whereby transitions to doubly excited levels become allowed.

The model can be extended to other dinuclear complexes but normally it will be necessary to use more than one parameter to describe the one-electron interaction.

For dinuclear complexes in which each of the metal ions has an orbital degenerate ground state the model may not predict a Landé interval rule for the antiferromagnetic coupling.

Note added in proof. After this manuscript was submitted for publication we became aware of the fact that a more general treatment than that of Jørgensen¹¹ has been given by Anderson²⁷ and also has been more clearly formulated by Owen and Thornley.²⁸

Acknowledgement. I thank Dr. C. E. Schäffer for encouraging this work and especially for discussions of the one-electron interaction.

REFERENCES

1. Schawlow, A. L., Wood, D. L. and Clogstan, A. M. *Phys. Rev. Letters* **3** (1959) 271.
2. Ferguson, J., Guggenheim, J. and Tanabe, Y. *J. Phys. Soc. Japan* **21** (1966) 692.
3. Hansen, A. E. and Ballhausen, C. J. *Trans. Faraday Soc.* **61** (1965) 631.
4. Schugar, H. J., Rossman, G. R., Thibeault, J. and Gray, H. B. *Chem. Phys. Letters* **6** (1970) 26.
5. Dexter, D. L. *Phys. Rev.* **126** (1962) 1962.
6. König, E. *Chem. Phys. Letters* **9** (1971) 31.
7. Jørgensen, S. M. *J. prakt. Chem.* **25** (1882) 341.

8. Kobayashi, H., Hasida, T., Kanda, E. and Mori, M. *J. Phys. Soc. Japan* **15** (1960) 1646.
9. Earnshaw, A. and Lewis, J. *J. Chem. Soc.* **1961** 396.
10. Pedersen, E. *Acta Chem. Scand.* **26** (1972) 333.
11. Jørgensen, C. K. *Absorption Spectra and Chemical Bonding in Complexes*, Pergamon, London 1962 p. 207; *Colloq. Int. Cent. Natl. Rech. Sci.* **180** (1969) 181.
12. Lindhard, M. and Weigel, M. *Z. anorg. allgem. Chem.* **299** (1959) 15.
13. Schwarzenbach, G. and Magyar, B. *Helv. Chim. Acta* **45** (1962) 1425.
14. Passerini, R. and Ross, I. G. *J. Sci. Instr.* **30** (1953) 274.
15. Schäffer, C. E. *J. Inorg. Nucl. Chem.* **8** (1958) 149.
16. Dubicki, L. and Martin, R. L. *Aust. J. Chem.* **23** (1970) 215.
17. Umshiyama, A., Nakahara, M. and Kando, Y. *Bull. Chem. Soc. Japan* **44** (1971) 2290.
18. Orgel, L. E. *J. Chem. Phys.* **23** (1955) 1824.
19. Yevitz, M. and Stanko, J. A. *J. Am. Chem. Soc.* **93** (1971) 1512.
20. Umshiyama, A., Nomura, T. and Nakahara, M. *Bull. Chem. Soc. Japan* **43** (1970) 3971.
21. Glerup, J. and Schäffer, C. E. In Cais, M., Ed., *Progress in Coordination Chemistry Proc. XI, I.C.C.C.*, Elsevier, Amsterdam 1968, p. 500.
22. Schäffer, C. E. *Pure Appl. Chem.* **24** (1970) 361.
23. Dunitz, J. D. and Orgel, L. E. *J. Chem. Soc.* **1953** 2594.
24. Griffith, J. S. *The Theory of Transition-Metal Ions*, Cambridge, At The University Press 1964, App. 2.
25. Heine, V. *Group Theory in Quantum Mechanics*, Pergamon, London 1964, p. 432 ff.
26. Watson, R. E. *Technical Report No. 12, June 15, 1959 Solid-State and Molecular Theory Group*, Massachusetts Institute of Technology, Cambridge, Mass.
27. Anderson, P. W. *Phys. Rev.* **115** (1959) 2.
28. Owen, J. and Thornley, J. H. M. *Rept. Progr. Phys.* **29** (1966) 675. (Part II.)

Received January 21, 1972.